Thermoreversible DMDBS Phase Separation in iPP: The Effects of Flow on the Morphology

Luigi Balzano,[†,⊥] Giuseppe Portale,[||,⊥] Gerrit W. M. Peters,[‡,⊥] and Sanjay Rastogi*[,†,§,⊥]

Department of Chemical Engineering and Department of Mechanical Engineering, Eindhoven University of Technology, P.O. Box 513, 5600 MB Eindhoven, The Netherlands, Institute of Polymer Technology and Materials Engineering (IPTME), Loughborough University, Loughborough, LE11 3TU, United Kingdom, DUBBLE CRG/ESRF, Netherlands Organization for Scientific Research (NWO), c/o ESRF BP 220, F-38043, Grenoble Cedex, France, Dutch Polymer Institute (DPI), PO Box 902, 5600 AX Eindhoven, The Netherlands

Received November 6, 2007; Revised Manuscript Received April 16, 2008

ABSTRACT: The crystallization rate of isotactic polypropylene (iPP) is often enhanced with sorbitol-based nucleating agents like 1,3:2,4-bis(3,4-dimethylbenzylidene)sorbitol or DMDBS. In the concentration range from the eutectic point (∼0.1 wt %) to 1 wt %, DMDBS crystallizes before the polymer, building a network of nanofibrils. The surface of this network hosts a large number of tailored nucleation sites that promotes the epitaxial nucleation of iPP. The formation of DMDBS fibrils corresponds to a liquid−solid phase separation that occurs on cooling, at a temperature T_c^{DMDBS}. On heating, DMDBS fibrils dissolve in iPP at a temperature $T_m^{DMDBS} > T_c^{DMDBS}$. For DMDBS contents less than 1 wt %, both T_c^{DMDBS} and T_m^{DMDBS} depend on the composition. We show that in the temperature window $T_c^{DMDBS} < T < T_m^{DMDBS}$ a percolated network of DMDBS fibrils is retained. This network can be broken with a shear flow that aligns the fibrils. At these high temperatures, iPP does not crystallize. Upon cooling, in the early stages of nucleation, the orientation of the fibrils is transferred to the lamellae because of the epitaxial relation between iPP and DMDBS. With this templating mechanism, we obtained well oriented crystalline morphologies of iPP after a shear pulse (shear rate of 60 s^{-1} applied for 3 s) at 185 °C for 0.3 wt %, at 195 °C for 0.7 wt % and at 210 °C for 1 wt % of DMDBS.

Introduction

Crystallization of semicristalline polymers, as for example isotactic polypropylene (iPP), is often speeded up with nucleating agents. These compounds increase the crystallization rate by promoting the formation of nuclei for crystal growth. More nuclei in the early stages of crystallization yield smaller crystallites at the end of the process. Such an alteration of the polymer morphology can have consequences on the properties of the material. Clarity and stiffness can be enhanced depending on the nature of the nucleating agent, its concentration and degree of dispersion.[1−4] During heterogeneous nucleation, the polymer nucleates at sites on the surface of the nucleating particles. Therefore, particles having a high specific surface offer a clear advantage. A wide range of substances are used as nucleating agents for iPP. Examples are salts of aromatic carboxylic acids (for instance sodium benzoate),[5,6] salts of phosphate esters (for instance NA-11),[7] and sorbitol derivatives.[8] The salts are insoluble in the polymer, and therefore, the specific surface is fixed by the particle shape. Moreover, their dispersion can be limited by the high viscosity of the matrix. In contrast, sorbitol derivatives dissolve in the polymer and the nucleating particles are formed with recrystallization from the melt. Dissolution and recrystallization provide a high degree of dispersion for these additives and the specific surface can be as high as 400 m^2/g.[9,10] As demonstrated by Lotz and coworkers,[9,11,12] successful nucleating agents for iPP have a crystalline structure and lattice parameters that match those of the polymer (epitaxy matching). In this paper, we discuss some aspects of flow effects on the morphology of the crystallizing iPP in presence of 1,3:2,4-bis(3,4-dimethylbenzylidene)sorbitol or DMDBS, the latest of the family of sorbitol-based nucleating agents. This compound is also known to be a good clarifying agent for iPP at concentrations lower than 1 wt %.[2,13] Clarification takes place because DMDBS increases dramatically the number of crystalline nuclei and leads to a reduction in the final size of the crystallites. iPP and DMDBS are miscible only at high temperatures. For concentrations less than 1 wt %, on cooling, DMDBS crystallizes before the polymer. This process can also be regarded as a liquid−solid phase separation of the binary mixture. Crystallization of DMDBS, driven by intramolecular hydrogen bonding,[14] leads to fibrils with a typical diameter of 10 nm and a typical length of hundreds of microns.[9] Starting from concentrations in the order of 0.1 wt %, these fibrils can also form bundles with a diameter up to 100 nm.[15] Due to a high aspect ratio, DMDBS fibrils entangle and give rise to a physical network[16,17] that can easily be broken with a shear flow that aligns the fibrils.[18]

DMDBS network intensifies the effects of the thermomechanical history on the morphology of iPP. In fact, the polymer lamellae grow in the direction orthogonal to the fibrils.[9,19,20] Hence, randomly oriented fibrils lead to isotropic iPP morphologies.[20] Whereas, fibrils prealigned with a flow lead to anisotropic polymer morphologies.[18]

Kristiansen et al.[2] investigated the phase diagrams of iPP−DMDBS mixtures during cooling and heating. They found that, during cooling, DMDBS crystallizes/phase separates at T_c^{DMDBS} and that, during heating, DMDBS melts, restoring the homogeneous mixture, at a temperature T_m^{DMDBS} sensibly higher than T_c^{DMDBS}. Both T_c^{DMDBS} and T_m^{DMDBS} depend on the composition. The rheological studies presented in this work suggest that, on heating, the network of DMDBS fibrils is retained for $T_c^{DMDBS} < T < T_m^{DMDBS}$. Therefore, we expect that a shear flow can align

* Corresponding author.
† Department of Chemical Engineering, Eindhoven University of Technology.
‡ Department of Mechanical Engineering, Eindhoven University of Technology.
§ Institute of Polymer Technology and Materials Engineering (IPTME), Loughborough University.
|| DUBBLE CRG/ESRF, Netherlands Organization for Scientific Research (NWO).
⊥ Dutch Polymer Institute (DPI).

10.1021/ma7024607 CCC: $40.75
Published on Web 06/21/2008

DMDBS fibrils and generate the condition for the growth of an oriented polymer morphology. Though it could be relevant for applications, the effect of flow at these high temperatures on the morphology is unexplored. The investigation of these effects is the aim of the present paper. Ultimately, we show that, making use of the thermoreversibility of the DMDBS phase separation, it is possible to choose thermomechanical histories allowing for the growth of an oriented iPP morphology after application of shear at temperatures as high as 210 °C.

2. Experimental Methods

Materials. The iPP used in this work is a commercial homopolymer grade from Borealis GmbH (Linz, Austria), labeled HD120MO, with molecular weight, M_w, of 365 kg/mol and polydispersity, M_w/M_n, of 5.4. DMDBS (Millad 3988) was obtained in powder form from Milliken Chemicals (Gent, Belgium) and used as received.

Sample Preparation. The polymer pellets were ground below the glass transition temperature and then mixed with DMDBS in a corotating twin screw mini-mixer (DSM, Geleen) for 10 min in a nitrogen-rich atmosphere, at temperatures ranging from 230 to 250 °C (the higher the DMDBS concentration the higher the compounding temperature). The mixture was compression molded with a hot press into films of different thicknesses: 1 mm for rheology and 200 μm for X-ray experiments. The molding temperature was 220 °C and the molding time was 3 min. The resulting films were quenched (∼100 °C/min) to room temperature and finally cut in disk-like samples. Three mixtures with 0.3, 0.7, and 1 wt % of DMDBS were prepared. For convenience, they are named B03, B07, and B1 respectively.

X-ray Characterization. Small angle X-ray scattering (SAXS) was performed at beamline BM26/DUBBLE of the European Synchrotron Radiation Facility (ESRF) in Grenoble, France. Time resolved images were recorded on a two-dimensional gas filled detector with 512 × 512 pixels and a pixel size of 260 μm × 260 μm. The detector was placed at approximately 6 m from the sample. The wavelength adopted was $\lambda = 1.24$ Å. Scattering and absorption from air were minimized by a vacuum chamber placed between sample and detector. SAXS images were acquired with an exposure time of 5 s and corrected for the intensity of the primary beam, absorption and sample thickness. The scattered intensity was integrated and plotted against the scattering vector, $q = (4\pi/\lambda)\sin\theta$ where 2θ is the scattering angle. Finally, the integrated intensity was defined as follows: $I_{Tot} = \int_{q_{min}}^{q_{max}} I(q)\, dq$, where q_{min} and q_{max} are the minimum and the maximum experimentally accessible q values respectively. Two dimensional SAXS images were also used for the characterization of anisotropic morphologies. For this purpose, three azimuthal regions are defined: (1) meridional, corresponding to the flow direction in real space; (2) equatorial, orthogonal to the meridional region; (3) diagonal, connecting the equatorial and meridional regions in the azimuthal direction.

Shear flow experiments in combination with SAXS were carried out using a Linkam Shear Cell (CSS-450) having Kapton windows. To erase previous thermomechanical histories, samples were always annealed at 240 °C for 3 min prior to the experiments.

Rheological Characterization. Rheological measurements were performed in the linear viscoelastic regime using a strain-controlled AR-G2 rotational rheometer (TA Instruments). In all cases a plate−plate geometry with a diameter of 8 mm was used. During the study of phase transitions, large strains can enhance the process and/or affect the morphology. Therefore, these experiments are carried out with strains within the linear viscoelastic window and as low as 0.5%.

DSC. The thermal effects of DMDBS phase separation was studied in quiescent conditions using a Q1000 calorimeter (TA Instruments). Samples of approximately 2 mg were placed into aluminum pans and tested in a nitrogen atmosphere. Recrystallization and melting of DMDBS within the iPP matrix was studied with the following protocol: (1) annealing at 240 °C for 3 min, then (2) cooling to 140 °C, and finally (3) heating to 240 °C. Both cooling and heating rate were set to 10 °C/min. Before analyzing the peaks, a linear baseline was subtracted from the raw data.

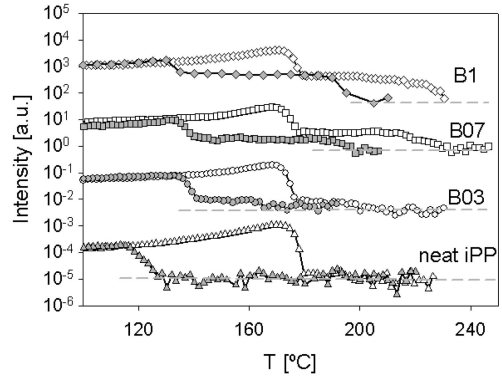

Figure 1. Integrated SAXS intensity as a function of the temperature during cooling (filled symbols) and during heating (open symbols) for the neat iPP, B03, B07, and B1. For visibility, curves are shifted in the vertical direction. The dashed lines represent the reference values at high temperatures.

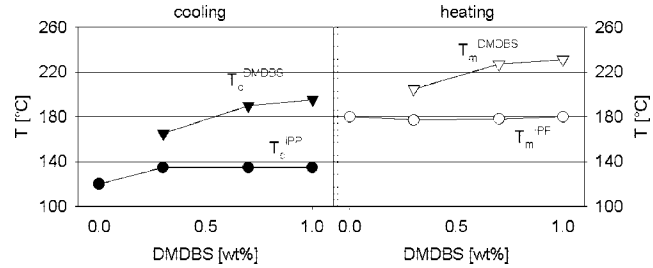

Figure 2. iPP−DMDBS phase diagrams obtained with SAXS on cooling (left) and on heating (right).

3. Results and Discussion

3.1. Phase Transitions in iPP−DMDBS Blends on Cooling and on Heating. iPP−DMDBS blends show a monotectic phase diagram during cooling and during heating for additive contents less than 1 wt %. As shown in Figure 1, quantitative information on these phase diagrams can be obtained with SAXS. During cooling (filled symbols), two increases of the total scattered intensity I_{Tot} indicate two phase transitions in the blends. The increase of I_{Tot} at high temperature corresponds to the crystallization/phase separation of DMDBS while that at low temperature corresponds to the crystallization of iPP. Analogously, during heating (open symbols), two decays in I_{Tot} indicate melting of the polymer (low temperature) and of DMDBS (high temperature). The temperatures characterizing the phase transitions of iPP and DMDBS during cooling and heating are summarized in the phase diagrams shown in Figure 2. For DMDBS contents up to 1 wt %, the crystallization and melting temperature of DMDBS (T_c^{DMDBS} and T_m^{DMDBS}) exhibits a dependence on the composition. Moreover, concentrations from 0.3 to 1 wt % of the additive lead to an increase in the crystallization temperature of the polymer (T_c^{iPP}) of ∼15 °C whereas the melting temperature (T_m^{iPP}) remains unchanged. In the range of concentration investigated (up to 1 wt %), the difference between T_c^{DMDBS} and T_m^{DMDBS}, i.e., the undercooling for crystallization of DMDBS within the molten iPP matrix, is on the order of 25 °C, independent of concentration. Similar values are reported in literature.[2] The phase separation of DMDBS leads to a percolated network of fibrils suspended in the polymer melt. As shown in Figure 3, the network causes large changes in the rheology of the system. During cooling from 240 to 150 °C (open symbols), at the onset of the phase separation, the storage modulus G' (at 5rad/s) rises noticeably.

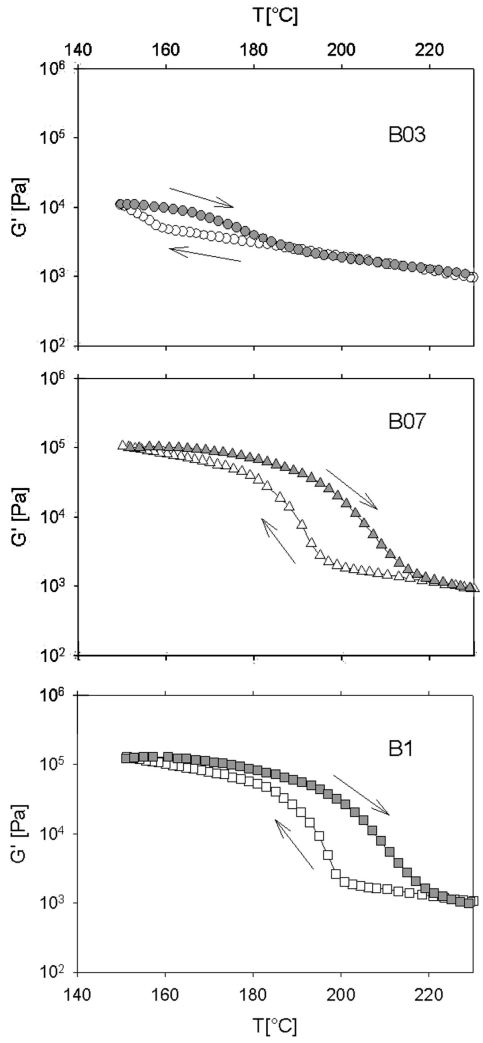

Figure 3. G' at 5rad/s as a function of the temperature on cooling from 240 to 150 °C (open symbols) and on heating from to 150 to 240 °C (filled symbols) for B03, B07, and B1.

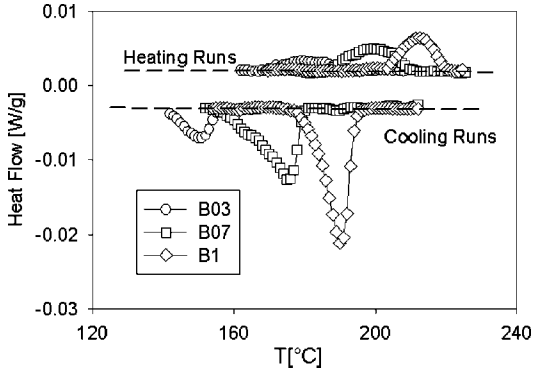

Figure 4. Thermal effects associated with the crystallization and melting of DMDBS within the iPP matrix. Higher DMDBS contents correspond to greater latent heats and to higher transition temperatures. The experiments are performed cooling from 240 to 150 °C and heating vice versa.

Table 1. Onset of Crystallization and Completion of Melting Temperatures of DMDBS in iPP Obtained with SAXS and DSC (10°C/min).

	T_c^{DMDBS} (°C)		T_m^{DMDBS} (°C)	
	SAXS	DSC	SAXS	DSC
B03	165	155	205	189
B07	190	180	227	207
B1	195	195	231	218

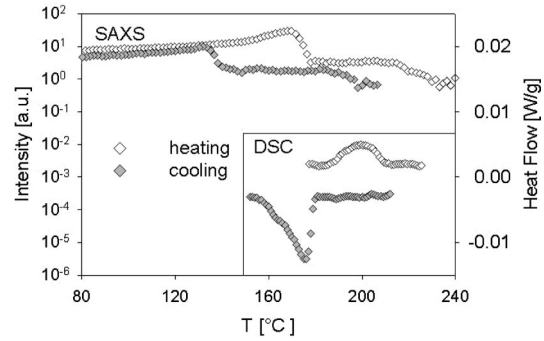

Figure 5. Comparison of SAXS and DSC during cooling and heating experiments on B07. SAXS experiments are performed cooling from 240 to 80 °C and heating vice versa. DSC experiments are performed cooling from 240 to 150 °C and heating vice versa.

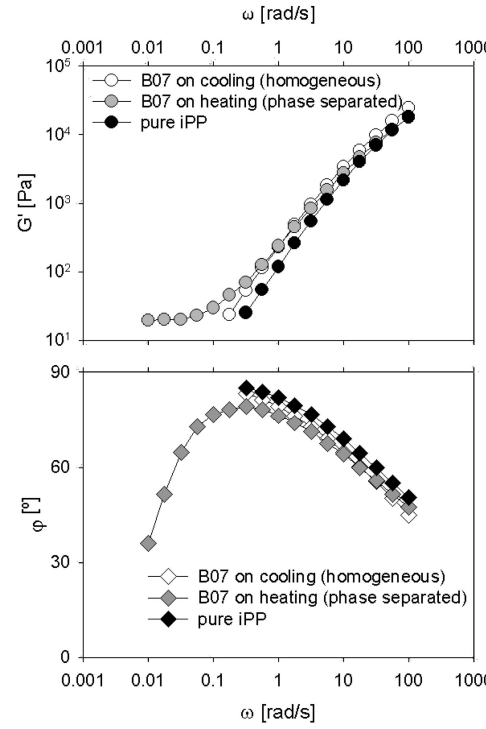

Figure 6. (Top) G' for B07 as a function of frequency at 205 °C. The neat polymer is used as a reference to evaluate the changes in B07 caused by two different thermal histories. In one case (white symbols), B07 is measured after cooling from 240 to 205 °C. In the other case (gray symbols), the same blend is measured after being cooled to 150 °C, heated to 205 °C and annealed at this temperature for 30 min (i.e., while it is in stable conditions at $T_c^{DMDBS} < T < T_m^{DMDBS}$).

Increasing the concentration, DMDBS phase separation shifts toward higher temperatures and so does the onset of G'. After completion of DMDBS phase separation, similar (temperature dependent) levels of G' are achieved for the blends B07 and B1 that are higher than for B03. The stiffer network formed at DMDBS concentrations higher than 0.3 wt % could be the result of the formation of more bundles of elementary fibrils. During heating from 150 to 240 °C (filled symbols), the temperature where G' recovers the high temperature value corresponds to the temperature where the DMDBS network redissolves into the melt. The network dissolution temperatures are close to T_m^{DMDBS} obtained with SAXS, indicating that the network is retained in (most of) the temperature window $T_c^{DMDBS} < T < T_m^{DMDBS}$.

Although only small amounts of DMDBS are used, by cooling from 240 to 150 °C and heating vice versa, the thermal effects

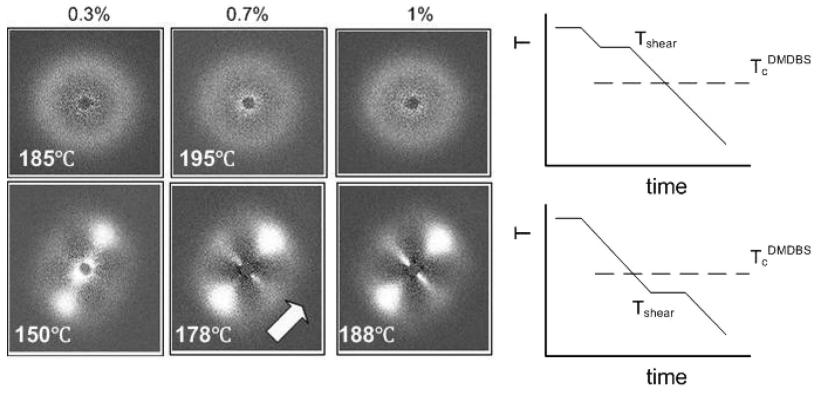

Figure 7. Two dimensional SAXS images recorded at room temperature for B03, B07 and B1 after the application of a shear (60 s^{-1} for 3 s) at the temperature indicated in the frame. The flow direction is indicated by the arrow.

associated to the phase transitions of DMDBS in the iPP matrix are large enough to be resolved with DSC. The thermograms are reported in Figure 4. The shift of the crystallization and melting temperature of DMDBS with the composition is consistent with SAXS and rheological data and, as expected, a greater latent heat is measured at larger DMDBS contents. Although the peaks are clearly visible, the latent heats are not reported as they are comparable with the detection limit of the equipment. Comparing DSC and SAXS data (see Figure 5 for the data of B07), it emerges that SAXS is more sensitive than DSC toward DMDBS phase separation. The transition temperatures determined with SAXS are, therefore, higher than those detected with DSC (see Table 1).

3.2. Effects of DMDBS Crystallization and Melting on Linear Viscoelasticity. From a linear-viscoelastic point of view, iPP−DMDBS blends, containing tiny amounts of the additive, behave like the usual melts when DMDBS is in solution, and similar to physical gels when DMDBS is phase separated.[21,22] In the temperature window $T_c^{DMDBS} < T < T_m^{DMDBS}$, a blend of iPP and DMDBS could behave in either way depending on the thermal history. In Figure 6, the linear viscoelastic behavior of the pure iPP is compared at 205 °C with that of the blend B07 for two different thermal histories. Note that for B07, $T_c^{DMDBS} < 205$ °C $< T_m^{DMDBS}$. In the first case (open symbols), before the measurement, B07 is cooled from 240 to 205 °C and annealed for 30 min at this temperature (thermal history 1, TH1). In the second case (filled symbols), before the measurement, B07 is cooled from 240 to 150 °C and then heated to 205 °C where it is annealed for 30 min (thermal history 2, TH2). The different thermal histories lead to a different behavior that can be explained considering the phase behavior of the blend (Figure 2). With the thermal history TH1, DMDBS is in solution during the measurement and, as expected, the rheological behavior of B07 is rather similar to that of the pure iPP. In contrast, with the thermal history TH2, DMDBS phase separates (at ∼190 °C) during cooling to 150 °C and does not redissolve when heated to 205 °C. The plateau of G' in the low frequency region ($\omega < 0.03$ rad/s) indicates that (part of) the network of DMDBS fibrils is retained. DMDBS fibrils, entangled with each other, have long relaxation times and can easily be aligned with a flow. This feature will be used in the following to generated highly oriented iPP morphologies after shear at relatively high temperatures.

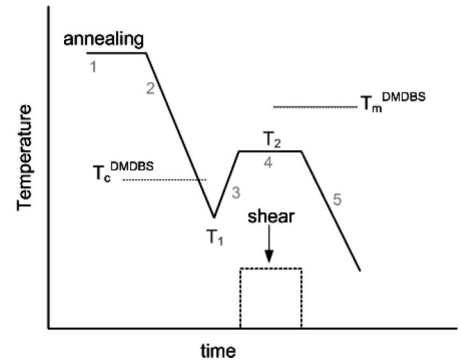

Figure 8. Schematic drawing of the thermal history designed to obtain oriented iPP morphologies after shear application at high temperatures. A shear pulse (60 s^{-1} for 3 s) is applied during stage 4. The design values of T_1 and T_2 for B03, B07, and B1 are given in Table 2.

3.3. iPP Crystallization after Shear at $T > T_c^{DMDBS}$. Because of the epitaxial relation, heterogeneously nucleated iPP lamellae grow orthogonally to DMDBS fibrils. Therefore, the crystalline morphology of the polymer reflects the orientation of DMDBS fibrils at the onset of crystallization. Figure 7 shows SAXS images obtained at room temperature after shear at the indicated temperature. The images in the top row correspond to a shear pulse (60 s^{-1} for 3 s) at $T > T_c^{DMDBS}$ (i.e., at 185 °C for B03, at 195 °C for B07, and at 210 °C for B1). While, the images in the bottom row correspond to a shear pulse (60 s^{-1} for 3 s) at $T < T_c^{DMDBS}$(i.e., at 150 °C for B03, at 178 °C for B07, and 188 °C for B1). When shear is applied at $T_{shear} > T_c^{DMDBS}$, iPP shows an isotropic morphology similar to what is observed for crystallization in quiescent conditions. In fact, when shear is applied, DMDBS is in solution with iPP; the fibrils form later, during the cooling, and grow with random orientations. In contrast, when the shear pulse is applied at $T_{shear} < T_c^{DMDBS}$, iPP exhibits a highly oriented morphology at room temperature. The shear deforms the DMDBS network causing alignment of

Table 2. Summary of the temperatures where shear is applied in the experiments of Figure 7 and of the choices made for the thermal history of Figure 8.

	flow before DMDBS phase separation (thermal history TH1)		flow after DMDBS phase separation (thermal history TH1)		parameters for the thermal history TH2		
	T_{shear} (°C)	iPP morphology at room temperature	T_{shear} (°C)	iPP morphology at room temperature	T_1 (°C)	T_2 (°C)	iPP morphology at room temperature
B03	185	isotropic	150	oriented	150	185	oriented
B07	195	isotropic	178	oriented	178	195	oriented
B1	210	isotropic	188	oriented	188	210	oriented

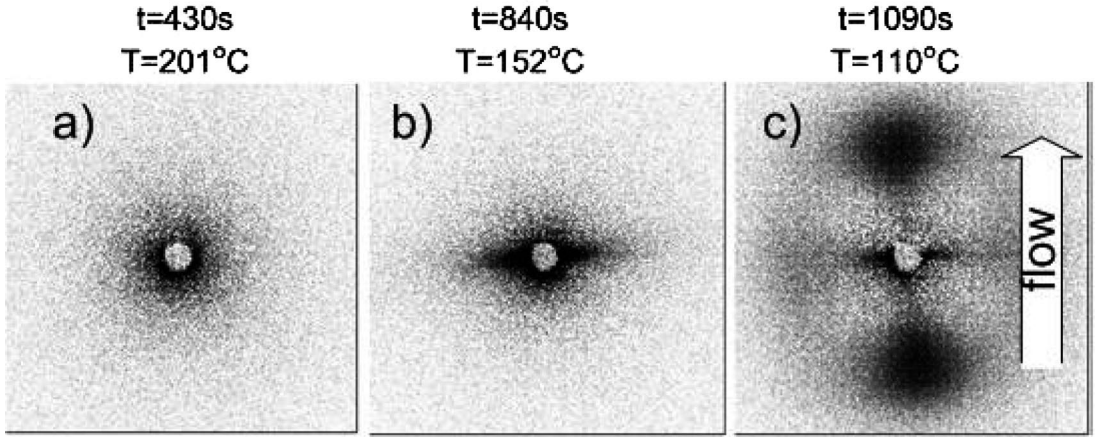

Figure 9. Time−temperature sequence of SAXS images for the blend B1 in the experiment illustrated in Figure 11. After shear application to the fibrillar network, the fibrils align and a streak of intensity appears at the equator. Crystallization of iPP at lower temperatures produces the meridional lobes. The flow direction is vertical.

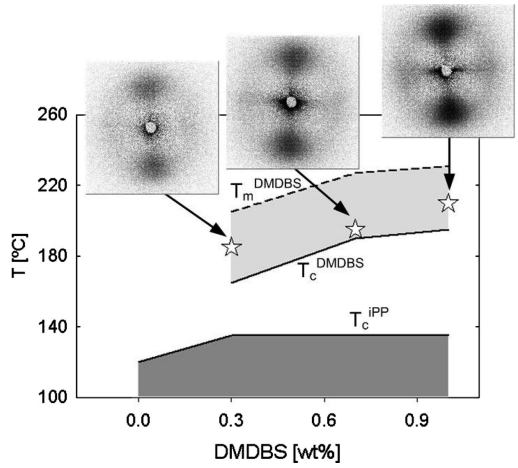

Figure 10. iPP−DMDBS phase diagram reporting the SAXS images corresponding to the room temperature morphology of iPP after application of shear (60 s^{-1} for 3 s) in the conditions indicated by the symbols (stars) and with the thermal history of Figure 8.

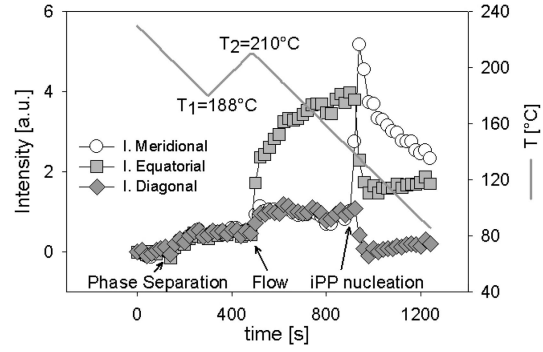

Figure 11. SAXS intensity for meridional, equatorial and diagonal part of the two-dimensional images as a function of time and temperature for the blend B1 subjected to shear (60 s^{-1} for 3 s) at 210 °C with the thermal history of Figure 8.

the DMDBS fibrils. In the early stages of iPP (heterogeneous) nucleation, the orientation of the fibrils is transferred to the polymer lamellae. Interestingly, for the temperature used in the top row of Figure 7, $T_c^{DMDBS} < T_{shear} < T_m^{DMDBS}$. Therefore, an oriented morphology can be obtained using the same mechanical history but a tailored thermal history (similar to TH2), see Figure 8. This thermal history includes the following steps: (1) Annealing at 240 °C for 3 min, (2) cooling at T_1 (below T_c^{DMDBS}), (3) heating to T_2 (below T_m^{DMDBS}), (4) application of a shear pulse (60 s^{-1} for 3 s), and finally, (5) cooling to room temperature. The temperatures T_1 and T_2 need to be chosen in relation with DMDBS concentration, the selected values are given in Table 2. SAXS images corresponding to the experiment with B1 are shown in Figure 9. After application of shear (image b), a streak in the intensity at the equator indicates the alignment of DMDBS fibrils with the flow direction. During cooling, these fibrils template a highly oriented iPP morphology (image c). Similar results are obtained for the blends B03 and B07, as summarized in Figure 10. More insight in the structure formation can be gained analyzing the SAXS intensities as a function of time/temperature. Figure 11 shows the results for B1. Cooling to $T_1 = 188$ °C causes phase separation of DMDBS ($T_c^{DMDBS} =$ 195 °C as determined by SAXS) and, as a consequence, the scattered intensity rises evenly in all the azimuthal areas. In the following step, heating to $T_2 = 210$ °C, the intensity remains constant indicating that the fibrils do not melt ($T_m^{DMDBS} =$ 224 °C). When the shear pulse is applied, DMDBS fibrils align with flow increasing the intensity scattered at the equator I_{eq}. Simultaneously, also the intensities scattered in the meridional and diagonal regions (I_{mer} and I_{diag}) raise, suggesting that flow promotes an extra phase separation with growth of randomly oriented fibrils. However, according to the lever rule, complete DMDBS phase separation is not possible at this high temperature and the process proceeds during the following cooling. The increase in I_{eq} rather than in I_{mer} and I_{diag} indicates that the growth of flow-oriented fibrils is favored over the growth of randomly oriented fibrils. At ∼140 °C, iPP nucleates and the growth of lamellae orthogonal to DMDBS fibrils takes place producing lobes in the SAXS meridional region. Epitaxially grown lamellae mitigate the density fluctuation between DMDBS and the matrix, hence the intensity scattered in equatorial and diagonal regions decreases.

4. Conclusions

Blends of iPP and DMDBS are miscible only at high temperatures. During cooling, DMDBS phase separates from the molten iPP at a temperature T_c^{DMDBS} that depends on the composition. With phase separation/crystallization of DMDBS a percolated network of nanofibrils is formed. In a previous paper,[18] we have shown that flow at $T < T_c^{DMDBS}$ can break the network and align DMDBS fibrils. The subsequent epitaxial (orthogonal) growth of iPP lamellae yields a highly oriented lamellar morphology. In this paper, we show that the same mechanism can be used also to obtain highly oriented iPP morphology after application of shear also at $T > T_c^{DMDBS}$. In

fact, when a phase-separated blend is heated, DMDBS fibrils redissolve in the polymer at a temperature $T_m^{DMDBS} > T_c^{DMDBS}$. Rheology suggests that in the temperature window $T_c^{DMDBS} < T < T_m^{DMDBS}$, the network of DMDBS fibrils is retained and application of a (shear) flow produces alignment of the fibrils. When the polymer is allowed to crystallize (decreasing the temperature) on this aligned template a highly oriented morphology is obtained.

Ultimately, we demonstrate that from understanding the phase behavior of iPP−DMDBS blends, on cooling and on heating, it is possible to design thermomechanical histories yielding highly oriented iPP morphologies after shear at relatively high temperatures (for instance 210 °C for 1 wt % of DMDBS), where viscosity is low.

Acknowledgment. The authors thank the personnel of BM26/DUBBLE and ID02 at ESRF (Grenoble) for their help during the X-ray experiments. Furthermore, NWO (Nederlandse Organisatie voor Wetenschappelijk Onderzoek) and ESRF are acknowledged for granting the beamtime. This work is part of the Research Programme of the Dutch Polymer Institute (DPI), PO Box 902, 5600 AX Eindhoven, The Netherlands, Project No. 132.6.

References and Notes

(1) Kristiansen, M.; Tervoort, T.; Smith, P.; Goossens, H. *Macromolecules* **2005**, *38*, 10461–10465.
(2) Kristiansen, M.; Werner, M.; Tervoort, T.; Smith, P.; Blomehofer, M.; Schmidt, H. W. *Macromolecules* **2003**, *36*, 5150–5156.
(3) Gahleitner, M.; Wolfschwenger, J.; Bachner, C.; Bernreitner, K.; Neissl, W. *J. Appl. Polym. Sci.* **1996**, *61*, 649–657.
(4) Lipp, J.; Shuster, M.; Feldman, G.; Cohen, Y. *Macromolecules* **2008**, *41*, 136–140.
(5) Zhu, P. W.; Tung, J.; Edward, G. *Polymer* **2005**, *46*, 10960–10969.
(6) Beck, H. N. *J. Appl. Polym. Sci.* **1967**, *11*, 673–685.
(7) Marco, C.; Ellis, G.; Gomez, M. A.; Arribas, J. M. *J. Appl. Polym. Sci.* **2002**, *84*, 1669–1679.
(8) Marco, C.; Ellis, G.; Gomez, M. A.; Arribas, J. M. *J. Appl. Polym. Sci.* **2002**, *84*, 2440–2450.
(9) Thierry, A.; Fillon, B.; Straupe, C.; Lotz, B.; Wittmann, J. C. *Prog. Colloid Polym. Sci.* **1992**, *87*, 28–31.
(10) Shepard, T. A.; Delsorbo, C. R.; Louth, R. M.; Walborn, J. L.; Norman, D. A.; Harvey, N. G.; Spontak, R. J. *J. Polym. Sci., Part B: Polym. Phys.* **1997**, *35*, 2617–2628.
(11) Fillon, B.; Lotz, B.; Thierry, A.; Wittmann, J. C. *J. Polym. Sci., Part B: Polym. Phys.* **1993**, *31*, 1395–1405.
(12) Alcazar, D.; Ruan, J.; Thierry, A.; Lotz, B. *Macromolecules* **2006**, *39*, 2832–2840.
(13) Tenma, M.; Mieda, N.; Takamatsu, S.; Yamaguchi, M. *J. Polym. Sci., Part B: Polym. Phys.* **2008**, *46*, 41–47.
(14) Wilder, E. A.; Spontak, R. J.; Hall, C. K. *Mol. Phys.* **2003**, *101*, 3017–3027.
(15) Lipp, J.; Shuster, M.; Terry, A. E.; Cohen, Y. *Langmuir* **2006**, *22*, 6398–640.
(16) Kobayashi, T.; Hashimoto, T. *Bull. Chem. Soc. Jpn.* **2005**, *78*, 218–235.
(17) Thierry, A.; Straupe, C.; Wittmann, J. C.; Lotz, B. *Macromol. Symp.* **2006**, *241*, 103–110.
(18) Balzano, L.; Rastogi, S.; Peters, G. W. M. *Macromolecules* **2008**, *41*, 399–408.
(19) Nogales, A.; Olley, R. H.; Mitchell, G. R. *Macromol. Rapid Commun.* **2003**, *24*, 496–502.
(20) Nogales, A.; Mitchell, G. R.; Vaughan, A. S. *Macromolecules* **2003**, *36*, 4898–4906.
(21) Dumitraş, M.; Friedrich, C. *J. Rheol.* **2004**, *48*, 1135–1146.
(22) Takenaka, M.; Kobayashi, T.; Saijo, K.; Tanaka, H.; Iwase, N.; Hashimoto, T.; Takahashi, M. *J. Chem. Phys.* **2004**, *121*, 3323–3328.

MA7024607